A&A 412, L11–L14 (2003)
DOI: 10.1051/0004-6361:20031667

Astronomy & Astrophysics

Confirmation of strong magnetic field amplification and nuclear cosmic ray acceleration in SN 1006

E. G. Berezhko[1], L. T. Ksenofontov[1,2], and H. J. Völk[3]

[1] Institute of Cosmophysical Research and Aeronomy, 31 Lenin Ave., 677891 Yakutsk, Russia
[2] Institute for Cosmic Ray Research, University of Tokyo, Chiba 277-8582, Japan
[3] Max Planck Institut für Kernphysik, Postfach 103980, 69029 Heidelberg, Germany

Received 4 September 2003 / Accepted 29 October 2003

Abstract. It is shown that the nonlinear kinetic model of cosmic ray (CR) acceleration in supernova remnants (SNRs) fits the shell-type nonthermal X-ray morphology, obtained in Chandra observations, in a satisfactory way. The set of empirical parameters is the same which reproduces the dynamical properties of the SNR and the spectral characteristics of the emission produced by CRs. The extremely small spatial scales of the observed X-ray distribution are due to the large effective magnetic field $B_d \sim 100\,\mu$G in the interior, which is also required to give a good fit for the spatially integrated radio and X-ray synchrotron spectra. The only reasonably thinkable condition for the production of such a large effective field strength is an efficiently accelerated nuclear CR component. Therefore the Chandra data confirm the inference that SN 1006 indeed accelerates nuclear CRs with the high efficiency required for SNRs to be considered as the main Galactic CR sources.

Key words. ISM: cosmic rays, supernova remnants – individual: SN 1006

A simple-minded calculation (McKenzie & Völk 1982) of the mean square magnetic field (MF) fluctuation $(\delta B)^2$

$$(\delta B/B)^2 = M_a P_c/(\rho_g V_s^2) \quad (1)$$

excited by the cosmic ray (CR) streaming instability in a strong shock with $M_a \gg 1$ shows that for efficient acceleration, $P_c \sim \rho_g V_s^2$, the excitation of resonant Alfvén waves is not only an important ingredient for the diffusive acceleration mechanism as such (Bell 1978; Blandford & Ostriker 1978). The resultant $(\delta B/B)^2 \gg 1$ could also imply a considerable obstacle for the theoretical description of the process up to the production of an enhanced effective MF in the acceleration region (Völk 1984). In Eq. (1) $M_a = V_s/c_a$ is the Alfvénic Mach number, where c_a denotes the Alfvén speed, P_c is the CR pressure at the shock front, and $\rho_g V_s^2$ is the ram pressure of the incoming plasma flow. The problem of Eq. (1) was taken up again recently by Bell & Lucek (2001), referring also to Lucek & Bell (2000) and attempting a nonlinear description of the MF evolution in a simple model, with the conclusion that a considerable amplification to what we shall call an effective MF should indeed occur. At the same time the selfconsistent treatment of the nonlinear time-dependent acceleration equations, both in theoretical and computational terms (e.g. Berezhko et al. 1996; Berezhko & Völk 1997), had progressed sufficiently to make quantitative modeling of CR acceleration in specific supernova remnants SNRs like the historical object SN 1006 possible (Berezhko et al. 2002), including the so-called injection process (Völk et al. 2003 and references therein). This allowed a detailed comparison with radio and X-ray observations which had become available in the nineties (Koyama et al. 1995; Allen et al. 2001), and allowed in particular a theoretical study of the morphology. In fact there are very recent measurements on details of the X-ray morphology of SN 1006 with Chandra (Long et al. 2003; Bamba et al. 2003). We shall show in this Letter that they confirm the amplification of the MF and – for lack of any acceptable alternative – its cause, the efficient acceleration of nuclear CRs.

Nonthermal X-ray observations indicate that at least CR electrons are accelerated in SNRs. In SN 1006 there is evidence that electrons reach energies of about 100 TeV (Koyama et al. 1995; Allen et al. 2001). Also TeV γ-ray emission from this source has been reported (Tanimori et al. 1998). However, depending on the assumed values for poorly known physical parameters in the theory (mainly the value of the MF and the nucleon injection rate, but also the ambient gas density), the observed high-energy γ-ray emission of SN 1006 could in principle be predominantly either simply the inverse Compton radiation of the synchrotron electrons scattering on the microwave background radiation as assumed by Tanimori et al. (1998), or π^0- decay emission due to hadronic collisions of CRs with gas nuclei (Berezhko et al. 2002). Comparing the synchrotron data with the calculated spectrum of the energetic electrons Berezhko et al. (2002) have inferred that the existing data require a very efficient acceleration of CR *nuclei* at the SNR blast wave (which converts about 10% of the initial SNR energy

Send offprint requests to: H. J. Völk,
e-mail: Heinrich.Voelk@mpi-hd.mpg.de

content into CR energy) as well as a large interior MF strength $B_{\rm d} \approx 120\ \mu$G. The large value of $B_{\rm d}$ is expected and possible in this case, using the spatially integrated radio and X-ray synchrotron spectra to empirically determine the MF strength and the injection rate in the theory. MF amplification was also one of the possibilities discussed later by Long et al. (2003). The nonthermal energy is distributed between energetic electrons and protons in the proportion 1.5×10^{-3}, similar to that of the Galactic CRs. From the point of view of acceleration theory this is the physically most plausible solution. It can also explain the peculiar dipolar structure of the synchrotron emission, with the dipole axis parallel to the ambient interstellar MF, as an effect of the homogeneity of the large-scale ambient MF (Völk et al. 2003), generally believed to exist in the rather clean interstellar environment of SN 1006 above the Galactic disk (Long et al. 2003). This morphology is fairly common among SNRs (Winkler & Long 1997). There is no alternative process without ad hoc-assumptions in the literature, or a new one which we could reasonably imagine, that would amplify the MF in a collisionless shock without particle acceleration. Nevertheless, the previous observations of the *large-scale* nonthermal emission in the case of SN 1006 did not strongly exclude a scenario which we called the "inefficient model", with low interior MF $B_{\rm d} \approx 10\ \mu$G in which nuclear CRs would play no important role and practically all nonthermal emissions would be of leptonic origin (Berezhko et al. 2002). As a corollary we shall show here that such a low-field scenario is not compatible with the local X-ray morphology.

For the comparison with the new Chandra data we shall not present the details of our model. They have been already described in the above paper (Berezhko et al. 2002). We shall rather use some simple analytical approximations, needed to qualitatively interpret the spatial distribution of the various CR components in SNRs. For the quantitative comparison we shall however use the exact numerical results. With some additions, the distribution of CRs produced by the spherically expanding shock of radius $R_{\rm s}$ and speed $V_{\rm s}$ can be roughly described by the steady state 1-dimensional transport equation for the CR distribution function $f(r,p,t)$

$$\kappa\frac{\partial^2 f}{\partial x^2} - u\frac{\partial f}{\partial x} + \frac{p}{3}\frac{{\rm d}u}{{\rm d}x}\frac{\partial f}{\partial p} - L = 0, \qquad (2)$$

where $x = R_{\rm s} - r$, and $u = V_{\rm s} - w$ is the speed of the scattering medium relative with respect to the shock front, w is the speed in the frame of the progenitor star, $\kappa(p)$ is the CR diffusion coefficient, p is particle momentum, L is a loss term, which we take in the simple form $L = f/\tau$, where τ is the loss time. Within this approach we neglect any effects of the shock modification due to the CR backreaction. Therefore the velocity profile has the form: $u(x<0) = u_1 = V_{\rm s}$; $u(x>0) = u_2 = u_1/\sigma$, where $\sigma = 4$ is the shock compression ratio. The solution of this transport equation is $f_i = f_0(p)\exp(-|x|/l_i)$ (Völk et al. 1981), where $f_0(p) = f(x=0,p)$ is the CR distribution function at the shock front and the scale

$$\frac{2\kappa_i}{u_i}\left[1-(-1)^i\sqrt{1+4\kappa_i/(u_i^2\tau_i)}\right]^{-1} \qquad (3)$$

describes the spatial CR distribution in the upstream ($i = 1$) and downstream ($i = 2$) regions, with simple limits for strong ($\tau_i \ll \kappa_i/u_i^2$) and weak ($\tau_i \gg \kappa_i/u_i^2$) losses. The CR distribution function at the shock front is determined by the expression

$$f_0 = Ap^{-q}\exp\left[-\int_{p_{\rm inj}}^{p}{\rm d}p\phi(p)/p\right], \qquad (4)$$

where $q = 3u_1/(u_1-u_2)$; $\phi = q[\kappa_1/(u_1^2\tau_1) + \kappa_2/(u_1u_2\tau_2)]$.

The losses produce two effects. First of all, the universal power law spectrum of accelerated CRs $f \propto p^{-q}$ has an exponential cutoff, where the maximum CR momentum $p_{\rm m}$ is determined through the condition $\phi(p_{\rm m}) = 1$. The losses lead also to a reduction of the spatial scales l_i that is essential in the cutoff region $p \sim p_{\rm m}$, cf. Eq. (4).

In the collisionless cosmic plasma, losses of nuclear CRs due to their interactions with the gas particles or with the ambient fields are negligibly small. The only important effects which restrict the proton acceleration are adiabatic cooling in the downstream region and a geometrical factor, that is the finite shock size. Formally compared with the simplified one-dimensional Eq. (2), the spherically symmetric transport equation contains the additional term $(2\kappa_1/r)(\partial f/\partial r)$ which contains the information about the shock size $R_{\rm s}$. Approximately we can write $\partial f/\partial r \approx -f/l_1$. Therefore this additional term in the plane wave approach can be expressed as a loss term L with the loss time $\tau_1 = R_{\rm s}/(2u_1)$. In the downstream region inside the SNR there is in addition also the term $(\nabla \boldsymbol{u}p/3)(\partial f/\partial p)$ which describes CR adiabatic cooling. It can be similarly estimated as a loss term with loss time $\tau_2 \sim R_{\rm s}/V_{\rm s}$. As a result, the upper proton momentum is determined by the relation $\kappa_1(p_{\rm m}) = R_{\rm s}V_{\rm s}/A$, where $A \sim 10$ (Berezhko 1996).

In addition to the above mechanical effects CR electrons suffer synchrotron losses with a time scale $\tau = 9m_{\rm e}^2c^2/(4r_0^2B^2p)$, where $m_{\rm e}$ is the electron mass, r_0 denotes the classical electron radius, and B is the MF strength. This is the dominant loss effect for our discussion. For sufficiently low MF, when the loss time τ exceeds the age t of the system, synchrotron losses are not important and the electron and proton spectra have exactly the same shape. In this case the highest energy electrons with $p \sim p_{\rm m}$ have quite a wide spatial distribution with scales $l_{1,2} \sim 0.1R_{\rm s}$. For high MF values the electron spectrum is restricted to significantly lower momenta, $p_{\rm m}^{\rm e} \ll p_{\rm m}$, than are protons. In this case accelerated electrons occupy only a very thin region around the shock front since $l_{1,2} \ll 0.1R_{\rm s}$ for all electron energies, for which $\tau \ll t$. The radio-electrons in the GeV range have $\tau \gg t$ and therefore $l_2 \sim 0.1R_{\rm s}$, consistent with observation (Long et al. 2003). The same is true for 100 TeV electrons which produce X-ray emission in the low-field case.

During the free expansion phase, preceding the early Sedov phase in which SN 1006 is at the present time, a Rayleigh-Taylor instability of the interface between the shocked interstellar gas and the ejected gas can occur (Gull 1973). It can make the downstream gas velocity profile $w(r)$ narrower than the classical Sedov profile, leading to an increase of the adiabatic expansion compared with the above estimate. As a result the radio emission profile may become somewhat narrower, whereas the X-ray emitting electrons are not affected, being dominated by the strong synchrotron losses

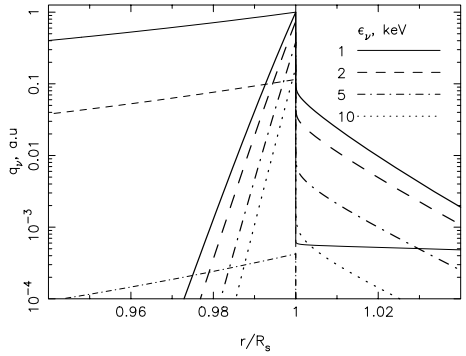

Fig. 1. Radial dependence of the X-ray emissivity at different X-ray energies. Thick and thin lines correspond to the efficient and the so-called inefficient model respectively.

around the shock. This instability can also locally amplify the MF. However, the unstable region moves to the deep interior ($r > 0.1R_s$) as the Sedov phase sets in, and dies out. Therefore we do not consider these processes any further. In particular they have no influence on the CR acceleration which occurs near the shock.

Our nonlinear model (Berezhko et al. 1996; Berezhko & Völk 1997) is based on a fully time-dependent solution of the CR transport equation together with the gas dynamic equations in spherical symmetry. It yields at any given distance r the momentum distribution $f(r, p, t)$ of CRs produced during the SNR evolution up to time t. Because of the efficient acceleration of the nuclear CR component (mainly protons), consistent with the expected injection rate of suprathermal particles into the acceleration process (Völk et al. 2003), the CRs significantly modify the shock structure by their nonlinear backreaction and amplify the MF (Berezhko et al. 2002). This MF amplification on all scales drives the CR scattering mean free path towards the particle gyroradius ρ_B, which means isotropic spatial diffusion. Since the particle distribution is also isotropic this implies the Bohm limit in the effective mean MF (Völk 1984): $\kappa = \rho_B v/3$, where v denotes the particle velocity. Figure 1 shows the calculated radial dependence of the X-ray synchrotron emissivity $q_\nu(\epsilon_\nu, r)$ (e.g. Berezinskii et al. 1990) for four X-ray energies $\epsilon_\nu = 1$, 2, 5 and 10 keV. One can see that the emissivity $q_\nu(r)$ peaks at the shock position $r = R_s$ because the radiating electrons have a sharp peak at $r = R_s$ due to the synchrotron losses. Since within the upstream and downstream emission regions the respective MF is approximately uniform, the spatial behavior of the emissivity $q_\nu(r)$ is determined by the spatial dependence of the CR distributions. According to Eq. (3), the expected upstream scale for the energy $\epsilon_\nu = 5$ keV is $l_1 = 0.01R_s$, taking into account that the upstream MF is $B_1 = \sigma_p B_0$, the upstream medium speed is $u_1 = V_s/\sigma_p$, $\sigma_p \approx 2$ is the precursor compression ratio, $V_s = 3200$ km s^{-1}, $R_s = 7.3$ pc, and $B_0 = 20$ μG is the MF in the shock precursor, i.e. the interstellar MF which is significantly amplified by the (nonlinear) CR streaming instability. This is in good agreement with the numerical results in Fig. 1, based on a source distance of 1.8 kpc.

The downstream scale due to the synchrotron losses, expected from relations (3), is $l_2 \approx \sqrt{\kappa_2 \tau_2} \approx 0.0037R_s$, taking into account the values $u_2 = V_s/\sigma$, $B_2 = \sigma B_0$, and $\sigma = 6.3$ (Berezhko et al. 2002). This agrees with the numerical values quite well. Due to the energy-independence of l_2, the spectral form of the downstream $q_\nu(\epsilon_\nu, r)$ does not depend on ϵ_ν (see Fig. 1, in agreement with observations (Bamba et al. 2003).

The MF $B_1 = B(r = R_s + 0)$, just ahead of the gas subshock at $r = R_s$, and the postshock MF $B_2 = B(r = R_s - 0)$ are connected by the relation $B_2 = \sigma_s B_1$, where $\sigma_s = 3.6$ is the subshock compression ratio. Since the upstream MF is significantly smaller than the downstream MF, the synchrotron emissivity undergoes a jump at $r = R_s$, and the emission from the downstream region significantly exceeds the upstream emission.

In projection along the line of sight, the radial emissivity profile determines the remnant's surface brightness. For the X-ray energy interval $\epsilon_1 < \epsilon_\nu < \epsilon_2$ it has the form

$$J_\nu(\rho) \propto \int_{\epsilon_1}^{\epsilon_2} \mathrm{d}\epsilon_\nu \int \mathrm{d}x q_\nu \left(\epsilon_\nu, r = \sqrt{\rho^2 + x^2}\right) \quad (5)$$

where ρ is the distance between the center of the remnant and the line of sight. It is clear from this expression that, due to the shock curvature, the surface brightness profile $J_\nu(\rho)$ differs from the emissivity profile $q_\nu(r = \rho)$, except for the simple case of a plane shock which is parallel to the line of sight. In particular, the position $\rho_m < R_s$ of the peak value $J_m = J_\nu(\rho_m)$ does not coincide with the shock edge $\rho = R_s$, and the scaling values $L_{1,2}$ which characterize the spatial brightness behavior in the inner ($\rho < \rho_m$) and the outer ($\rho > \rho_m$) regions are not simply the downstream and upstream emissivity scales $l_{1,2}$.

The numerically calculated brightness profile for the X-ray energy interval between $\epsilon_1 = 2$ keV and $\epsilon_2 = 10$ keV is shown in Fig. 2. The brightness profile is characterized by the outer scale $L_1 = 0.002R_s = 0.015$ pc which comes from the emission of the downstream region alone, and from the shock curvature. The inner brightness scale is $L_2 \approx 7L_1 = 0.1$ pc.

The sharpest experimental X-ray brightness profiles obtained by the Chandra observers (Long et al. 2003; Bamba et al. 2003) are shown in Fig. 2. Since the absolute values of the measurements are not known, all theoretical and experimental profiles are normalized to their peak values. One can see that the experimental values agree very well with our calculations. All other observed brightness profiles are significantly wider: on average $L_1 = 0.04$ pc and $L_2 = 0.2$ pc (Bamba et al. 2003). There are several reasons for a broadening of the observed profile, compared with the ideal case of a spherical shell. First of all, it is clear from the observations that the actual shock front deviates from a spherical form. The wavy shape of the shock front can be produced as the result of a small scale density inhomogeneity of the ambient interstellar medium. Any small scale distortion of the spherical emission shell leads to a broadening of the observed brightness profile.

It is important to note that there is direct experimental evidence that not only the inner part ($\rho < \rho_m$) of the brightness distribution $J_\nu(\rho)$ but also the outer part ($\rho > \rho_m$) is due to emission from the downstream region $r < R_s$, in contrast to the arguments of Bamba et al. (2003). At the gas subshock the density increases by a factor $\sigma_s = 3.6$ and the gas temperature increases by a factor of 9.3. Due to this fact the thermal

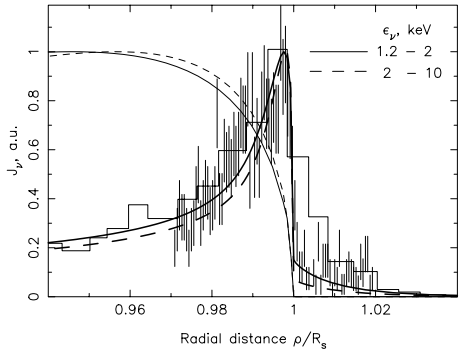

Fig. 2. Projected radial dependence of the X-ray brightness in the 1.2 to 2 keV (solid) and 2 to 10 keV (dashed) X-ray energy interval. Thick and thin lines correspond to the efficient and the so-called inefficient model respectively. The Chandra data, corresponding to the sharpest profile, are shown by the histogram (Long et al. 2003) and the vertical dashes (Bamba et al. 2003).

emission from the upstream region is small compared to the downstream thermal emission. Therefore, if the observed nonthermal X-ray emission $J_\nu(\rho)$ at $\rho > \rho_m$ is due to the upstream electrons, then one should expect that the thermal X-ray radiation has a peak value at a smaller distance than ρ_m and drops to almost zero at $\rho = \rho_m$, if as before ρ_m represents the peak position of the nonthermal X-ray emission (in other words the peak of the thermal X-rays is expected in this case at smaller distances). However, the observed peak positions of the thermal and nonthermal X-ray emissions and their shapes in the outer region $\rho > \rho_m$ are almost identical (Bamba et al. 2003). This is a strict confirmation that the entire observed X-ray emission comes from the downstream region, exactly as predicted by Berezhko et al. (2002).

In Figs. 1 and 2 we also present calculations for the so-called inefficient model. Of course, the number of accelerated electrons was chosen to be consistent with the observed synchrotron emission for the assumed downstream MF $B_d = 16\,\mu$G (see Berezhko et al. 2002 for details). Since in this case the MF is much lower, so that synchrotron losses play no role, the upstream (negligible brightness) and downstream electron length scales $l_{1,2} \sim 0.1 R_s$ are so large (see Fig. 1) that the brightness profile is almost two orders of magnitude wider than observed. The clear conclusion is that inefficient scenarios for CR injection/acceleration in SN 1006 should be rejected since they strongly contradict the X-ray measurements.

Note that in order to form such a sharp decrease of their distribution towards the center of the remnant one needs a powerful loss process in the downstream region, independently of what specific acceleration process produces the energetic electrons near the SN shock. Adiabatic cooling, as it was demonstrated, is not strong enough. In the diluted ionized plasma the only known strong electron loss process is synchrotron losses. But this process can influence the 100 TeV electron distribution in a significant form only if the downstream MF is as high as $B_d \sim 100\,\mu$G, much larger than the typical interstellar MF. Such a high MF can be created due to CR backreaction upstream of the shock. For such a large downstream MF $B_d \sim 100\,\mu$G the number of relativistic electrons consistent with the observed radio flux from SN 1006 is so low (Berezhko et al. 2002) that they are not able to create Alfvén waves with sufficiently high amplitudes $\delta B \sim B$. Indeed, taking into account that a typical value of the Alfvén speed is $c_a = 20\,\mathrm{km\,s^{-1}}$ and that for $B_d \sim 100\,\mu$G the pressure of the CR electron component $P_{c1} \approx 10^{-3}\rho_g V_s^2$ (Berezhko et al. 2002), we have $(\delta B/B)^2 \approx 0.1$ from Eq. (1), which implies an insignificant background MF amplification. The only possibility is efficient proton acceleration. In this case their number, consistent with all existing data, is so high, $P_c \sim \rho_g V_s^2$, that they are able to strongly amplify the MF and at the same time to provide efficient CR scattering approaching the Bohm limit (Bell & Lucek 2001). Such a MF amplification is required by the comparison of our selfconsistent model with the synchrotron observations. We note that the uniformity of the downstream MF strength distribution during the Sedov phase, despite the strong expansion of the downstream region, is a direct consequence of the temporal weakening of the random MF generation at the shock $B_2 \propto V_s^2$ (Bell & Lucek 2001), if we can approximate the MF as being isotropic according to the relation $B_d^2 \rho_g^{-4/3} = \mathrm{const}$. (e.g. Chevalier 1974).

We conclude that these data confirm the MF amplification and the efficient acceleration of nuclear CRs in SN 1006, predicted by Berezhko et al. (2002). This efficiency is consistent with the requirements for the Galactic CR energy budget.

This work has been supported in part by the Russian Foundation for Basic Research (grant 03-02-16325). EGB and LTK acknowledge the hospitality of the Max-Planck-Institut für Kernphysik, where part of this work was carried out. LTK acknowledges the receipt of a JSPS Research Fellowship.

References

Allen, G. E., Petre, R., & Gotthelf, E. V. 2001, ApJ, 558, 739
Bamba, A., Yamazaki, R., Ueno, M., & Koyama, K. 2003, ApJ, 589, 827
Bell, A. R. 1978, MNRAS, 182, 147
Bell, A. R., & Lucek, S. G. 2001, MNRAS, 327, 433
Berezhko, E. G. 1996, Astropart. Phys., 5, 367
Berezhko, E. G., Elshin, V. K., & Ksenofontov, L. T. 1996, JETP, 82, 1
Berezhko, E. G., & Völk, H. J. 1997, Astropart. Phys., 7, 183
Berezhko, E. G., Ksenofontov, L. T., & Völk, H. J. 2002, A&A, 395, 943
Berezinskii, V. S., Bulanov, S. A., Dogiel, V. A., Ginzburg, V. L., & Ptuskin, V. S. 1990, Astrophysics of cosmic rays, ed. V. L. Ginzburg (North-Holland, Amsterdam), 1
Blandford, R. D., & Ostriker, J. P. 1978, ApJ, 221, L29
Chevalier, R. A. 1974, ApJ, 188, 501
Gull, S. F. 1973, MNRAS, 161, 47
Koyama, K., Petre, R., Gotthelf, E. V., et al. 1995, Nature, 378, 255
Long, K. S., Reynolds, S. P., Raymond, J. C., et al. 2003, ApJ, 586, 1162
Lucek, S. G., & Bell, A. R. 2000, MNRAS, 314, 65
McKenzie, J. F., & Völk, H. J. 1982, A&A, 116, 191
Tanimori, T., Hayami, Y., Kamei, S., et al. 1998, ApJ, 497, L25
Völk, H. J. 1984, High Energy Astrophysics, ed. J. Tran Thanh Van (Gif sur Yvette: Éditions Frontières)
Völk, H. J., Berezhko, E. G., & Ksenofontov, L. T. 2003, A&A, 409, 563
Völk, H. J., Morfill, G. E., & Forman, M. A. 1981, ApJ, 249, 161
Winkler, P. F., & Long, K. S. 1997, ApJ, 491, 829